HHS Public Access

Author manuscript

*Comb Chem High Throughput Screen*. Author manuscript; available in PMC 2017 January 01.

Published in final edited form as:

*Comb Chem High Throughput Screen*. 2016 ; 19(5): 412–422.

# Selection of Lung Cancer-Specific Landscape Phage for Targeted Drug Delivery

**James W. Gillespie**, **Lixia Wei**, and **Valery A. Petrenko**

Department of Pathobiology, College of Veterinary Medicine, Auburn University, AL 36849

## Abstract

Cancer cell-specific diagnostic or therapeutic tools are commonly believed to significantly increase the success rate of cancer diagnosis and targeted therapies. To extend the repertoire of available cancer cell-specific phage fusion proteins and study their efficacy as navigating moieties, we used two landscape phage display libraries f8/8 and f8/9 displaying an 8- or 9-mer random peptide fusion to identify a panel of novel peptide families that are specific to Calu-3 cells. Using a phage capture assay, we showed that two of the selected phage clones, ANGRPSMT and VNGRAEAP (phage and their recombinant proteins are named by the sequence of the fusion peptide), are selective for the Calu-3 cell line in comparison to phenotypically normal lung epithelial cells and distribute into unique subcellular fractions.

### Keywords

Drug Delivery; Endocytosis; Landscape Phage Display; Lung Cancer; NGR motif

## Introduction

Respiratory neoplasms remain a significant health problem in the United States accounting for an estimated 14% of new cancer cases and approximately 30% of cancer mortalities for both men and women [1]. Lung cancer is classified into two major groups based on observed histological differences: non-small cell lung cancer (NSCLC) and small cell lung cancer (SCLC) [2]. Both NSCLC and SCLC display a high level of heterogeneity within the tumor [3] that may limit successful therapeutic responses due to a small population of cells escaping the effects of treatment and causing recurrent diseases demonstrating resistance to the treatment. Several strategies have been suggested to overcome drug resistance and decrease undesired side effects by the use of precision medicines or ‘magic bullets’, a concept pioneered by Paul Ehrlich, to deliver lethal concentrations of drug to cancer cells before resistance develops [4,5]. The use of nanomedicines, encapsulated forms of existing drugs, has shown to significantly increase the therapeutic index of existing drugs and concurrently reduced dose-limiting side effects. Commonly, nanomedicines accumulate at

**Corresponding Author:** Dr. Valery A. Petrenko, Ph.D., Sc.D., 253 Greene Hall, Department of Pathobiology, College of Veterinary Medicine, Auburn University, AL 36849, USA. Phone: (334) 844-2897; Fax: (334) 844-2652; petreva@auburn.edu.

**Conflict of Interest Statement**

The authors declare that the research was conducted in the absence of any commercial or financial relationships that could be construed as a potential conflict of interest.

the site of tumor pathology due to the enhanced permeation and retention (EPR) effect, which involves their passive diffusion through vascular defects commonly associated with rapidly forming blood vessels in certain tumor types. [6]. Although significant progress has been achieved with passive targeting, chemotherapy resistance and tumor relapse are still observed clinically in a number of cancer types. It was demonstrated that the tumor-specific effects achieved by passive targeting can be enhanced by attachment of nanomedicines with targeting molecules specifically interacting with receptors expressed on cancer cells and cancer vasculature to create actively targeted nanomedicines [5,7]. Since the tumor microenvironment has been shown recently to be more complex than previously believed, actively targeted nanomedicines have failed to show significant improvements compared to their passively targeted counterparts. As the poorly understood biological and technical barriers that limit the precise delivery of drug to the site of disease are identified, actively targeted nanomedicines with desired functional activites can be designed. A limited number of ‘smart’ navigating and targeting ligands with specific cancer cell binding and penetrating activity have been identified to address these barriers. Therefore, a need for novel ligands and novel drug navigation strategies remains a challenge for adequate active tumor targeting and drug delivery.

Phage display [8] has been used extensively over the past three decades for generation of peptide and protein ligands interacting with cellular components or surface receptors across a wide range of diverse sources including isolated molecules, intact bacterial cells, and mammalian cells (*in vitro*, *in vivo*, or *ex vivo)*. In particular, vectors based on filamentous bacteriophages of the class Ff (M13, fd, and f1), supporting a variety of different display formats depending on the host protein used, have been used extensively for displaying foreign peptides and proteins [8]. Structurally, filamentous phage consist of a small, ~9 kb single-stranded, circular genome surrounded by 5 structural proteins (pIII, pVI, pVII, pVIII, and pIX) to produce long, filamentous particles [9]. Phage display on the Ff class of bacteriophage vectors has produced numerous libraries with large structural complexities on the order of $\geq 10^9$ unique sequences. These libraries contain a number of constrained and/or randomized structures which provide a rich source of targeting ligands for numerous applications [8,10]. Thus, phage display in minor coat protein p3 has been used to identify cancer specific peptides for a variety of tumor types including lung cancer [11].

Landscape phage libraries of type f8 [10,12,13] designed on the filamentous bacteriophage vector fd-tet, consist of a collection of phage with random inserts introduced at the N-terminal end of every copy of the pVIII major coat protein of the phage vector and are subsequently expressed in ~4,000 copies across the length of the phage particle (Figure 1A). This layout dramatically alters the physical properties of the phage surface so that each phage particle is structurally unique compared to the remainder of the library and each phage possesses a specific ability to interact with the surrounding environment. In contrast to display on the p3 protein, the multivalent display of foreign peptides on the p8 protein allows easy identification of families containing homologous phage binders and select phages with desirable cell binding or penetrating propensities[14–16]. Landscape phage virions are an ideal targeting material compared to traditional antibodies as large quantities of pure phage or phage proteins can be produced inexpensively and very rapidly while retaining high product purity and shelf-storage stability. Numerous platforms derived from

the cancer cell-selective phage proteins and their fusion peptides have been developed over the past decade for various diagnostic and therapeutic applications. These platforms, reviewed elsewhere [17], include targeted nanoparticles for gene delivery to specific cells [18,19], probes for diagnostics and imaging [20–23], cancer-specific liposomes or micelles containing various therapeutic payloads [24–26], cancer-specific siRNA nanoparticles [27], and nanorods for photothermal therapy [28,29]. Given the wide number of platforms being targeted with phage display-derived peptides, there is an increasing need for diverse collections of targeting ligands that possess tumor cell specificity and also capable of intracellular delivery.

We aimed to develop a comprehensive panel of phage proteins with fusion peptides specific towards a representative NSCLC cell line, which could be used for construction of targeted anticancer nanomedicines and studying their activity as imaging probes and therapeutics. We explored the Calu-3 cell line derived from a metastatic site in a patient receiving prior chemotherapy to mimic the advanced stage disease commonly treated as a recurrent or metastatic disease. In this study, we used previously characterized 8- and 9-mer landscape phage display libraries f8/8 and f8/9 as a source of novel protein ligands identified against an advanced stage NSCLC cell line *in vitro* to expand the collection of available ligands with specificity to NSCLC molecular subtypes. Our molecular selection schemes are specifically developed to identify ligands that possess a desired outcome – for example, the ability of a ligand to bind cancer cell receptors, penetrate and accumulate into subcellular compartments, and ultimately produce the expected cytotoxic effect when loaded with appropriate drugs. We were able to identify two novel phage clones containing a commonly identified NGR motif that display unique cellular distributions that should be studied further using our previously developed active-targeting nanomedicine platforms.

## Materials & Methods

### Cells

All cell lines were purchased from the American Type Culture Collection (ATCC, Manassas, VA) as a frozen vial and maintained as described in the technical bulletins. All cell passages were cultured in 25-$cm^2$ cell culture treated flasks (Corning, Corning, NY) in a humidified 37°C incubator with 5% $CO_2$. Cells were subcultured when they reached 80–90% confluence by trypsin-EDTA treatment and reseeded at a density of ~$4\times10^4$ cells/$cm^2$.

### Phage Display Libraries

As a source of diverse binding ligands we used multibillion clone landscape phage display libraries f8/8 and f8/9, constructed from the fd-tet type vectors f8-1 and f8-6 [30], which respectively display an 8- or 9-mer peptide fusion at the N-terminus of every copy of the pVIII major coat protein [10,13]. Phage derived from these landscape libraries have a 55 amino acid mature pVIII major coat protein sequence of $NH_2$-A**XXXXXXXX**[**D/X**]PAKAAFDSLQASATEYIGYAWAMVVVIVGATIGIKLFKKFTSKAS-COOH rather than a 50 amino acid wild-type protein, where X can be any random amino acid (coded by NNK codons, where N is any base and K is G or T bases). The 10th position of the pVIII protein fusion is D for phage derived from the 8-mer library and X for phage derived from

the 9-mer library. Herein, we commonly identify phage by their fusion peptide sequence, however all protein references refer to the full-length, 55 amino acid protein sequence unless specified otherwise. All general phage handling, propagation, purification, titering, and DNA sequencing procedures have been described previously [31]. The number of phage particles was estimated using either spectroscopy to measure the number of physical phage particles (virions) or by titering phage in a bacterial host as colony forming units (CFU). Physical titering of phage was performed when phage concentrations were higher than $10^{11}$ virions/mL by measuring the absorbance at 269 nm and converted to vir/mL by the following formula for f8/8 and f8/9 libraries (9198 nucleotide genome) as derived previously [12]:

$$1 \text{ Absorbance Unit } (\text{AU})_{269} = 6.5 \times 10^{12} \text{ virions/mL}$$

## Selection of Lung Cancer Specific Phage

**(A) First Round—**Calu-3 and SAE cells were cultured in 25-$cm^2$ flasks until ~90% confluent. An aliquot of each library containing $1.2\times10^{11}$ virions, with each unique fusion sequence being represented by ~100 copies, was diluted in blocking buffer (0.5% BSA + EMEM with 10% FBS) and transferred to an empty, cell culture treated 25-$cm^2$ flask for one hour incubation at room temperature to remove phage binding to the treated plastic. Unbound phage were recovered and transferred to a flask that had been treated overnight with EMEM/10% FBS for one hour at room temperature to remove medium and serum binding phage. The f8/8 library underwent a single round of serum depletion, while the library f8/9 underwent two rounds of serum depletion. The unbound phage were recovered and then incubated with normal lung airway epithelial cells (SAE cells) for 1 hour at room temperature. The resulting depleted libraries were then transferred to flasks containing target Calu-3 lung cancer cells and allowed to incubate for one hour at room temperature. Cells were washed and phage recovered as in section C.

**(B) Second to Fourth Rounds—**For further rounds, an aliquot of $1\times10^{11}$ virions from each of the eluate and lysate sublibraries generated from the previous round was incubated with confluent Calu-3 cells in EMEM with 10% FBS in an incubator at 37°C and 5% $CO_2$ for 1 hour. A schematic of selection is presented in Figure 1B. Cells were washed and phage recovered as in section C.

**(C) Washing and Sublibrary Generation—**Unbound phage were recovered from the flasks and saved for titering. The Calu-3 cells were washed ten times with cold washing buffer (0.1% Tween 20/0.5% BSA in EMEM) for 5 minutes each to remove low binding phage. Washes were collected and saved for titering. Surface bound phage were recovered by addition of elution buffer (200 mM glycine, pH 2.2/0.1% BSA in EMEM) followed by neutralization with neutralizing buffer (1 M Tris-HCl, pH 9.1). Adherent cells were washed with washing buffer two times at room temperature and collected as “post-elution washes” for titering. The remaining cell monolayers were scrapped from the bottom of the culture flask and transferred to a centrifuge tube. Cells were pelleted and the remaining cell pellets were lysed with lysis buffer (2% w/v sodium desoxycholate/10 mM Tris-HCl, pH 8.0/2 mM

EDTA) for 10 minutes at room temperature to isolate internalized phage. Recovered surface bound and post-elution wash phage were concentrated to ~0.2 mL with Amicon 100 kDa MWCO concentrators (EMD Millipore, Billerica, MA). Concentrated phages from eluate and post-elution wash fractions were combined as a single eluate sublibrary. Phage from eluate and lysate sublibraries were infected into K91BluKan *E. coli* cells, amplified, and purified by PEG/NaCl precipitation the following day for future rounds of selection. All recovered fractions were titered and quantified as described previously [31].

**(D) Sequencing of Sublibraries—**A portion of the amplified library was spread on an NZY/Tet agar plate after 45 minutes of growth and placed in an in 37°C incubator overnight. Individual clones were gridded on NZY/Tet agar plates and incubated at 37°C overnight. The sequence of gpVIII was amplified by PCR as described previously [31]. PCR products were purified and sequenced by dye-terminator sequencing at the Massachusetts General Hospital (MGH) DNA Core (Cambridge, MA). Unique clones were propagated in 2 mL scale and concentrated by a double PEG/NaCl precipitation for storage and future experiments.

## Computational Analysis

The gpVIII sequence from unique phage clones was translated to their corresponding pVIII protein sequences using the EditSeq tool found within the DNASTAR, ver. 11 (Madison, WI) suite of molecular biology analysis programs. Phage clones were manually curated for common structural motifs and subsequently grouped into families of related peptide motifs based on an identified consensus motif. Unique phage clones isolated from both phage libraries were analyzed for information content using the INFO tool found within the RELIC suite of programs designed for the statistical analysis of combinatorial peptide libraries such as the two phage libraries studied here [32]. A histogram showing the relative change in information content between both libraries was constructed by subtracting the relative abundance of information observed at a given information content in the selected library from the relative abundance of information observed in a random sampling of the unselected phage libraries. The overall diversity of the two libraries before and after four rounds of selection was calculated using the AADIV tool also found within the RELIC suite of programs.

Using MimoDB (ver. 4.2, updated April 2014), a manually curated, publicly accessible database of peptides identified following selection with random phage display libraries [33], unique phage clones that we identified were submitted to the optimized MimoDB BLAST tool designed for identification of conserved structural motifs within short peptides and compared to the latest released version of the database. Resulting peptide motifs identified following selection against other cancer cell lines or known cell surface receptors were manually compiled into a single table and conserved peptide motifs were grouped and reported in Supplemental Figure 1.

## Phage Capture Assay - Selectivity and Specificity

The ability of unique phage clones to bind to their target lung cancer cell line, Calu-3, in comparison to other control cells and serum was studied by a phage capture assay described

previously [34]. In this assay, small airway epithelial cells were used as phenotypically normal lung epithelial cells and MCF-7 breast cancer cells were used as non-related cancer cells. Briefly, $5\times10^4$ cells per well of each cell type was plated in triplicate for each phage in a 96-well plate in EMEM and allowed to grow to 90% confluence. Triplicate wells containing EMEM was also prepared for each phage clone to be used as a negative control. After overnight incubation, cells were washed for 1 hour with serum-free medium at room temperature. Individual phage clones were added to corresponding wells at ~$10^6$ CFU per well in blocking buffer (0.5% BSA in EMEM) for 1 hour in a 37°C/5% $CO_2$ cell culture incubator. Unbound phage were removed by washing with washing buffer (0.5% BSA/0.1% Tween 20 in EMEM) for 5 minutes for a total of eight washes. Cells were lysed with CHAPS (3-[(3-Cholamidoproply)dimethylammonio]-1-propanesulfonate) lysis buffer (2.5% CHAPS/0.5% BSA in EMEM) for 10 minutes with gentle shaking on a rocker. The remaining cell lysis was then titered for phage with K91BluKan *E. coli*. A previously identified phage displaying an unrelated peptide, VPEGAFSSD that binds streptavidin [35], was used as a negative control in all assays. Phage recovery was calculated as the ratio of recovered phage versus the input phage as follows:

$$\text{Percent Recovery } (\%) = \frac{\text{Phage}_{\text{ Output}}}{\text{Phage}_{\text{Input}}} \times 100$$

### Phage Capture Assay - Mode of Interaction

Interactions between phage clones displaying a fusion peptide with high target specificity and their target Calu-3 cells were studied by tracking the uptake of intact phage particles. Phage capture assay was performed as above, however phage bound to the surface were recovered by eluting with elution buffer (200 mM glycine, pH 2.2/0.1% BSA in EMEM), neutralized with neutralizing buffer (1 M Tris-HCl, pH 9.1), and saved for titering. Cells were then washed twice with washing buffer and saved for titering. The remaining cell monolayer was lysed with lysis buffer to recover internalized phage and saved for titering. All recovered fractions were titered as described previously [31]. Recoveries were reported as a percentage of the total number of input phage. Cell uptake percentages were calculated as the number of phage recovered in a particular fraction by the sum of all recovered phage from all fractions as follows:

$$\text{Percent Recovered }_{\text{fraction}}(\%) = \frac{\text{Phage }_{\text{fraction}}}{\text{Phage}_{\text{eluate}} + \text{Phage}_{\text{PEW}} + \text{Phage}_{\text{lysate}}} \times 100$$

## Results

### Selection of Lung Cancer Cell-Specific Phage

To identify a collection of the most prominent phage proteins that interact specifically with novel or aberrantly overexpressed receptors of unknown identity present on the surface of an advanced stage NSCLC cell line, Calu-3, we used two proprietary landscape phage libraries that display a randomized 8- or 9-mer fusion peptide in the N-terminus of every copy of the pVIII major coat protein of fd-tet phage. These libraries consist of phage containing random

DNA oligomers inserted into a specific region of the pVIII gene of the wild-type phage. This fusion allows the translated peptide to be expressed at the N-terminus of the mature major coat protein, pVIII. When phage from these libraries are propagated, they express ~4,000 copies of a single, modified protein containing a fusion between the protein encoded by the randomized DNA insert and the N-terminus of the wild-type pVIII major coat protein as described in more detail [24].

To identify phage particles that interact specifically with Calu-3 cells, we first removed phage interacting with unrelated targets such as: 1) plastic, 2) cell culture medium, 3) serum components, and 4) phenotypically normal lung cells. After these depletion steps, we enriched each phage library for phage interacting at room temperature with the surface receptors of a NSCLC cell line, Calu-3, and separated the binding phage into eluate and lysate library fractions that would theoretically contain cell surface-binding and cell-internalizing phage respectively, as depicted in the flow chart in Figure 1. As expected, we saw a moderate recovery of phage from the eluate fractions of both libraries (Figure 2A) and lower recovery of phage from the lysate fractions (Figure 2B) for the first round of selection.

To increase the stringency of the following rounds of selection, we increased the temperature of phage incubation from room temperature to a more physiologically relevant temperature of 37°C as depicted in the flow chart (Figure 1B). We hypothesized that the increase in temperature would increase the yield of the phage recovered in the lysate fraction, irrespective of input library used, due to increased endocytosis and other metabolically active transport mechanisms. This leads to enrichment of our phage library for Calu-3 cell line specific phage that are internalized by active transport mechanisms. Beginning with the second round of selection, the input was prepared by combining eluate fractions prepared in the previous round of selection as depicted in Figure 1. For example, the eluate input was prepared as a combination of phage from both eluate and lysate fractions. We observed an approximate 10-fold increase in phage recovery for each subsequent round of selection for both fractions in both libraries (Figure 2A/B), with the exception for the final round of selection with the f8/9 library lysate fraction that resulted in a slight decrease in recovered phage. These results suggest enrichment of the recovered phage population for the peptide sequences that interact specifically with the target Calu-3 cell line. The significant enhancement of phage yield recovered in the lysate fraction after increasing the incubation temperature may suggest that active transport mechanisms are probably used to increase intracellular phage penetration.

Approximately 100 clones from each library were sequenced after four rounds of selection to identify the corresponding fusion peptide sequence of each recovered phage clone and determine the overall diversity present in the libraries after selection. Several families of phage containing common linear motifs were identified with the f8/8 library (Table I) and with the f8/9 library (Table II). Also a few common motifs between both libraries were identified, including EPG[Q/E], NGR, RGD and DGR, most families were unique within their respective library of origin due to the differences in amino acid diversity in each library before selection. We isolated a family of sequences containing the motif DxDY[S/T] that had been identified in previous screening of an 8-mer phage library against the MCF-7 breast cancer cell line [34] suggesting a possible common receptor between the two types of

cancer. We also selected a phage clone, VEEGGYIAA, isolated during selection against lung cancer cells, that had also been reported previously in selection against breast cancer [34] and pancreatic cancer cells [36] using the same library suggesting a common receptor between all three cancer types. These 'promiscuous' phages [37], discovered recently in our selection experiments, have a good prospect of being used as targeting ligands against different cancer cell types.

After selection with the f8/8 library, we observed a common EPG[Q/E] motif that was enriched in 18% (5/28) of the total unique sequences identified. We have seen previously that phage clones containing an EPGX motif often interact non-specifically with an unidentified component in serum. From these results, we sought to reduce the number of serum-binding clones isolated during screening of the f8/9 library. To accomplish this, we performed a second step of serum depletion during the selection scheme of the f8/9 library. After four rounds of selection with the f8/9 library, we observed only 4% (2/47) of clones containing this motif suggesting an enhanced depletion of serum-binding clones during depletion.

To estimate the library complexity following our selection scheme and identify functionally significant clones, we used the RELIC suite of statistical analysis programs which was developed specifically for the analysis of combinatorial peptide libraries such as the two landscape phage libraries used in this study. Briefly, the information content of any random phage displayed peptide can be generally defined as the probability of an amino acid appearing following selection versus the probability of the amino acid appearing by chance in an unselected library in a defined position. Thus phage with high information content contain a fusion peptide with amino acids statistically underrepresented in the unselected library and often indicate the presence of a selective pressure to maintain the rare amino acid. We next sought to determine the change in total information associated with each phage library before and after four rounds of selection against the Calu-3 NSCLC cell line. It was hypothesized that following selection, there would be an enrichment of phage clones with high information content and a decrease in phage clones with low information content. After four rounds of selection with the f8/8 library against the Calu-3 cell line, 30 unique phage clones were analyzed for their information content compared to a collection of 73 random, unselected clones from the f8/8 library. We observed a decrease in phage with low information content and a decrease in some phage with moderate information content. We also observed a significant increase in some moderate information containing phage as well as an increase in high information content phage (Figure 2C, solid line). Overall, selection with the f8/8 library produced clones with higher information content than the unselected population suggesting a successful selection experiment and enrichment of lung cancer specific phage in the generated output library.

Similarly, we analyzed 53 unique phage clones recovered after four rounds of selection with the f8/9 library and compared them to a collection of 64 random clones from the unselected f8/9 library. We observed a much larger decrease in moderate information containing phage as well as a much larger increase in high information content phage (Figure 2C, dashed line). We also noticed a slight increase in low information content phage compared to an

unselected population. Again our results suggest there was an enrichment of lung cancer specific phage clones in the f8/9 library.

Another common characteristic used to measure the quality and utility of a phage display library is the calculation of the peptide diversity also referred to as the completeness of sequence representation within the libraries. We next determined the observed protein diversity of our two generated libraries (composed of the eluate and lysate clones after the fourth round of selection) using the AADIV tool found in the RELIC analysis suite. We hypothesized that following selection there should be a decrease in the overall population diversity compared to an unselected library due to the selective enrichment of cell-binding motifs identified through the selection procedure and a loss of non-specific peptides. There was a 2.42 fold decrease in overall peptide diversity from $9.14\times10^{-3} \pm 4.49\times10^{-3}$ in the unselected f8/8 library to $3.77\times10^{-3} \pm 2.76\times10^{-4}$ ($P < 0.0001$) following four rounds of selection against the Calu-3 lung cancer cell line. Similarly, there was a 4.51 fold decrease in overall peptide diversity from $2.67\times10^{-3} \pm 1.44\times10^{-3}$ in the unselected f8/9 library to $5.93\times10^{-4} \pm 3.53\times10^{-4}$ ($P < 0.0001$) following four rounds of selection. After selection, there was a significant decrease in overall diversity per amino acid from 55.6% to 37.3% in the f8/8 library and from 51.8% to 43.8% in the f8/9 library. From these data, we show that there was enrichment of both phage libraries for clones with high information content and a decrease in overall amino acid diversity as expected following selection against our target cells. As suggested previously [10], each of the two f8-type libraries biopanned here occupy different sequence spaces resulting in different populations of ligands following the same selection protocol.

## Interaction of Phage with the Target Lung Cancer Cell Line

Ideal ligands for targeted drug delivery should have the ability to interact specifically with their target cancer cells and avoid phenotypically normal cells surrounding the tumor. To determine if the enrichment of phage clones observed during our final round of selection produced Calu-3 cell-specific phage clones, we used a phage capture assay. In Figure 3A, we present the binding specificities of a representative collection of identified phage clones from the f8/8 and f8/9 libraries. Clones were screened from the f8/9 library according to their associated information content compared to an unselected library (Table III). As expected, all representative clones showed a statistically significant increase in binding to Calu-3 cells compared to a non-related phage containing the guest fusion sequence of VPEGAFSSD, which was shown previously to have an affinity to streptavidin and possess little ability to bind cancer cells ($P < 0.0001$). The ratio of phage yield (output/input) obtained for each clone bound to Calu-3 cells by phage yield of non-related phage (VPEGAFSSD) is referred to as a phage's specificity. Alternatively, for each clone the ratio of phage yield to Calu-3 cells by yield to another cell line is referred to as a phage's selectivity. A number of clones studied showed minimal binding to normal lung epithelial cells or serum components (high specificity), however some of the phage clones identified from the f8/9 library showed equal or better binding to serum under identical conditions. Clones such as VNGRAEAP, DTSLTTDE, and DESISYIDQ show specific interactions with only the target Calu-3 cells ($P < 0.0001$). Some identified clones such as EVNVEEINL, and DAGPMWSG, show moderately high interaction with the target cells and possess the ability

to interact with other non-related cancer cells more than normal cells (Tukey-Kramer HSD test, non-related cancer vs. normal cells; $P = 0.0198$ and $P < 0.0001$ respectively). However some phage clones, like ARPILSSE, were shown to have moderately high interactions with the target cells (Tukey-Kramer HSD test, target vs. non-related cancer cells, $P < 0.0001$), but also showed minor interacts with a non-related cancer type and phenotypically normal cells that were statistically equally to each other. (Tukey-Kramer HSD test, non-related cancer vs. normal cells; $P = 0.0587$). We also observed that some clones, such as ANGRPSMT, ASPLAAPA, DAGPMWSG, and GTADQDYS, were selective to a non-related breast cancer cell line, MCF-7, when compared to a non-related phage described in materials section ($P < 0.0001$). Two prominent phage clones that showed high relative selectivity and specificity at the studied concentration were ANGRPSMT and VNGRAEAP that both contain a conserved NGR motif shown to interact with aminopeptidase N (CD13), a commonly overexpressed marker on tumor cells and vascular endothelium around tumor tissues [38].

Most drug delivery applications requiring a cell-specific ligand not only need to discriminate the desired target cell from a collection of normal cells, but also have the property of being internalized for successful treatment. We therefore sought to determine the relative uptake distribution for a select number of Calu-3 cell-specific phages. We hypothesized that selective phage clones would undergo different mechanisms of transport based on the specific interaction between their fusion peptide and their currently unidentified receptors. To determine a general subcellular distribution of phage probes, we studied the interaction of intact phage with Calu-3 cells using a modified phage capture assay in which phage were recovered from phage-treated cells using different extraction buffers. Phage were split into three representative subcellular fractions as performed during selection (eluate, post-elution wash, and lysate) and titered. From the studied phage clones, there were three distinct classes of phage interactions observed with lung cancer cells: 1) clones that predominately bind to the surface of the cells and remain restricted to the cell surface; 2), clones that are internalized and associate with an internal membrane or membrane bound organelle; and 3) clones that internalize and remain in the cytoplasm (Figure 3B–D).

The first class of phage was represented by phage clones, DNGTFREM and ASPLAAPA, which show greater than 70% of phage recovery in the eluate fraction (Figure 3B). We hypothesize that these phage clones interact with surface restricted receptors that do not undergo endocytosis or have a slow rate of endocytosis, which leads to minimal phage uptake. The second class of phage was represented by phage clone, ANGRPSMT, which showed greater than 50% of phage recovery in the lysate fraction and <10% recovery in the eluate fraction (Figure 3C). We hypothesize that these phage either interact with receptors that undergo rapid endocytosis or are able to directly penetrate through the cell membrane upon interaction with a surface receptor. We also hypothesize that this class of phage clones are internalized and protected from the post-elution washes by a membrane bound organelle or other hydrophobic compartment/membrane. The third and most common class of phage clones was represented by phage clones: ARPILSSE, DAGPMWSG, VNGRAEAP, GTADQDYS, and DPTGTSAP, which were identified by a composition of ~40% of phage recovered in the eluate fraction, ~5% in the lysate fraction, and ~60% in the post-elution wash fraction (Figure 3D). We hypothesize that this class of phage interacts with a receptor that undergoes endocytosis and resides primarily in the cytoplasm of the cells. It was shown

previously that phage recovered from the post-elution wash fractions are released from the cytoplasm after activation of phospholipases during pH shock, resulting in membrane defects and subsequent release of internalized phage [39]. The observed rapid cytoplasmic release can also be contributed to the instability of the endosomal membrane after accumulation of certain phage particles during intracellular trafficking that leads to the collapse and subsequent leakage of infectious phage particles from the endosomal compartment to the cytoplasm. This endosomal escape activity of phage proteins was demonstrated previously by Wang et al. for phage proteins with the fusion peptide DMPGTVLP that were incorporated into liposomal nanomedicines [40]. Nanoparticles that enhance endosomal escape and avoid degradation of their encapsulated payload are rapidly becoming a requirement for nanomedicines and the identification and classification of ligands that promote endosomal escape is an important consideration for effective ligand selection in many therapeutic applications.

## Discussion

Phage display libraries containing a rich collection of highly diverse molecular probes are commonly used in affinity selection protocols to identify protein sequences with high affinity and selectivity to a desired target, in a rapid and economical manner. Neoplastic cells, including lung cancer cells, often are represented by cells with different molecular phenotypes leading to different cell surface receptors being expressed across the cellular landscape. This cellular landscape can also be affected by differences in local tumor microenvironment following chemotherapy and/or radiotherapy treatments leading to a more complex cell surface. Due to the dynamic nature of the cellular landscape, identification of a suitable selection scheme and cellular targets is important for the improvement of tumor-specific therapeutics or diagnostics.

Here, we used a subtractive selection scheme to identify a collection of fusion peptides with selectivity towards a lung cancer cell line, Calu-3, previously receiving chemotherapy before isolation from a metastatic site, in comparison with phenotypically normal cells. Identification of cancerous cells that may have received previous chemotherapy and/or also may have metastasized away from the primary lesion still remains a challenge. The phage, their fusion proteins, and foreign peptides identified from our library would be ideal candidates for detection and targeted cancer chemotherapy applications as demonstrated previously [41]. Lung cancer cell-specific peptides have been isolated by other groups from pIII phage display libraries displaying 12-mer [42] or 20-mer [43,44] peptide sequences within the five copies of the mature pIII protein. The pVIII landscape phage display library format, rather than modification of the pIII protein commonly used with other phage display libraries, provides a unique molecular landscape across the length of the surface of each phage formed by the patterning of thousands of identical copies of each selected fusion peptide sequence. A comparison of affinity between selected phage from both types of libraries has been described elsewhere [45], with phage identified from landscape libraries often displaying higher affinities in the sub-nanomolar Kd range due, in part, to the density of ligands within each phage. We recently showed that a landscape phage, displaying a breast cancer cell-specific peptide (DMPGTVLP) directed towards cell surface expressed nucleolin, had an affinity in the picomolar range (Kd = $1.3\times10^{-12}$ M) to its target MCF-7

breast cancer cell line [34] suggesting the high propensity of landscape phage libraries to generate high affinity targeting probes against important targets for anticancer therapy [46].

Using a previously developed phage capture assay, recovered phage clones were screened in their target cell line to determine how they interact with the cells. One noted limitation of our phage capture assay is that we are only able to identify intact, infective phage particles. This could slightly alter the elution profiles of each phage due to phage degradation by proteases at physiological temperatures or collapse of phage structure intracellularly. This limitation is unlikely given the highly stable structure of phage particles and the short incubation time of phage with mammalian cell targets. Using the information content generated from the RELIC analysis, we were able to hypothesize that phage with high relative information content would bind specifically with our target cells. This information content statistic could allow for identification of phage likely to interact with a given target compared to the unselected library and provide an ideal starting point for selectivity experiments following a final round of selection that may result in a large number of highly diverse structural families. However, using this statistic to replace selectivity experiments is not recommended, as the degree of selectivity or specificity towards a given target is not included in the calculation. For example from the f8/9 clones presented, DESISYIDQ showed to be highly selective producing a specificity ratio of 14.01 from an information content of 25.029, however EVNVEEINL was less selective with a specificity ratio of only 3.31 from a higher relative information content of 28.245 (Table III).

As shown with the common RGD motif, neighboring peptides surrounding a shared structural motif can modulate the binding or activity of the RGD motif with surface integrins as proposed previously [47]. We also show here a similar effect was observed with an NGR motif. Structurally the NGR motif was located in the same position on each of the studied phages (A**NGR**PSMT and V**NGR**AEAP), however the selectivity and subcellular distribution were consistently different between the two phages. One clone, VNGRAEAP, showed dramatic cell specificity and was commonly found within the cytoplasm of Calu-3 cells. Alternatively, ANGRPSMT, showed more broad reactivity with cancer cells and found predominately in membrane bound organelles or endosomes. Thus we suggest here that these neighboring residues are hypothesized to increase the affinity or specificity of the parent motif as well as modulate cell signaling and other regulatory events within the cell after binding [48]. It was suggested previously that multiple functional domains within a selected peptide may also be enriched during the selection procedure that results in modified binding specificity or changes in functional activity [37]. We believe that the panel of unique landscape phages and their proteins that are specific and selective to this NSCLC cell line, Calu-3, can be easily adapted for any of the existing analytical and therapeutic platforms. Reviewed in [17].

## Supplementary Material

Refer to Web version on PubMed Central for supplementary material.

## Acknowledgments

**Funding**

This work was supported by the National Cancer Institute at the National Institutes of Health [U54 CA151881 to V.A.P.] and the Auburn University Research Initiative in Cancer (AURIC). The content is solely the responsibility of the authors and does not necessarily represent the official views of the National Institutes of Health.

## References

1. Siegel R, Ma J, Zou Z, Jemal A. Cancer Statistics, 2014. CA Cancer J Clin. 2014; 64:9–29. [PubMed: 24399786]
2. Vescio RA, Connors KM, Bordin GM, Robb JA, Youngkin T, Umbreit JN, Hoffman RM. The Distinction of Small Cell and Non-Small Cell Lung Cancer by Growth in Native-State Histoculture. Cancer Res. 1990; 50:6095–6099. [PubMed: 2168289]
3. Fraire AE, Roggli VL, Vollmer RT, Greenberg SD, McGavran MH, Spjut HJ, Yesner R. Lung Cancer Heterogeneity. Prognostic Implications. Cancer. 1987; 60:370–375. [PubMed: 3594372]
4. Modok S, Mellor HR, Callaghan R. Modulation of Multidrug Resistance Efflux Pump Activity to Overcome Chemoresistance in Cancer. Curr Opin Pharmacol. 2006; 6:350–354. [PubMed: 16690355]
5. Markman JL, Rekechenetskiy A, Holler E, Ljubimova JY. Nanomedicine Therapeutic Approaches to Overcome Cancer Drug Resistance. Advanced Drug Delivery Reviews. 2013; 65:1866–1879. [PubMed: 24120656]
6. Torchilin V. Tumor Delivery of Macromolecular Drugs Based on the EPR Effect. Advanced Drug Delivery Reviews. 2011; 63:131–135. [PubMed: 20304019]
7. Neri D, Bicknell R. Tumour Vascular Targeting. Nat Rev Cancer. 2005; 5:436–446. [PubMed: 15928674]
8. Smith GP, Petrenko VA. Phage Display. Chem Rev. 1997; 97:391–410. [PubMed: 11848876]
9. Marvin DA, Symmons MF, Straus SK. Structure and Assembly of Filamentous Bacteriophages. Prog Biophys Mol Biol. 2014; 114:80–122. [PubMed: 24582831]
10. Kuzmicheva GA, Jayanna PK, Sorokulova IB, Petrenko VA. Diversity and Censoring of Landscape Phage Libraries. Protein Eng Des Sel. 2009; 22:9–18. [PubMed: 18988692]
11. McGuire MJ, Gray BP, Li S, Cupka D, Byers LA, Wu L, Rezaie S, Liu Y-H, Pattisapu N, Issac J, Oyama T, Diao L, Heymach JV, Xie X-J, Minna JD, Brown KC. Identification and Characterization of a Suite of Tumor Targeting Peptides for Non-Small Cell Lung Cancer. Sci Rep. 2014; 4:4480. [PubMed: 24670678]
12. Kuzmicheva GA, Jayanna PK, Eroshkin AM, Grishina MA, Pereyaslavskaya ES, Potemkin VA, Petrenko VA. Mutations in Fd Phage Major Coat Protein Modulate Affinity of the Displayed Peptide. Protein Eng Des Sel. 2009; 22:631–639. [PubMed: 19633313]
13. Petrenko VA, Smith GP, Gong X, Quinn T. A Library of Organic Landscapes on Filamentous Phage. Protein Eng. 1996; 9:797–801. [PubMed: 8888146]
14. Ivanenkov VV, Menon AG. Peptide-Mediated Transcytosis of Phage Display Vectors in MDCK Cells. Biochem Biophys Res Commun. 2000; 276:251–257. [PubMed: 11006114]
15. Ivanenkov VV, Felici F, Menon AG. Targeted Delivery of Multivalent Phage Display Vectors Into Mammalian Cells. Biochim Biophys Acta. 1999; 1448:463–472. [PubMed: 9990298]
16. Ivanenkov V, Felici F, Menon AG. Uptake Intracellular Fate of Phage Display Vectors in Mammalian Cells. Biochim Biophys Acta. 1999; 1448:450–462. [PubMed: 9990297]
17. Petrenko, VA.; Smith, GP. Phage Nanobiotechnology. Royal Society of Chemistry; 2011.
18. Gandra N, Wang D-D, Zhu Y, Mao C. Virus-Mimetic Cytoplasm-Cleavable Magnetic/Silica Nanoclusters for Enhanced Gene Delivery to Mesenchymal Stem Cells. Angew Chem Int Ed Engl. 2013; 52:11278–11281. [PubMed: 24038718]
19. Mount JD, Samoylova TI, Morrison NE, Cox NR, Baker HJ, Petrenko VA. Cell Targeted Phagemid Rescued by Preselected Landscape Phage. Gene. 2004; 341:59–65. [PubMed: 15474288]
20. Deutscher SL. Phage Display in Molecular Imaging and Diagnosis of Cancer. Chem Rev. 2010; 110:3196–3211. [PubMed: 20170129]
21. Lang Q, Wang F, Yin L, Liu M, Petrenko VA, Liu A. Specific Probe Selection From Landscape Phage Display Libraryand Its Application in Enzyme-Linked Immunosorbent Assay of Free Prostate-Specific Antigen. Anal Chem. 2014; 86:2767–2774. [PubMed: 24533565]

22. Han L, Liu P, Petrenko VA, Liu A. A Label-Free Electrochemical Impedance Cytosensor Based on Specific Peptide-Fused Phage Selected From Landscape Phage Library. Sci Rep. 2016; 6:22199. [PubMed: 26908277]
23. Yin L, Luo Y, Liang B, Wang F, Du M, Petrenko VA, Qiu H-J, Liu A. Specific Ligands for Classical Swine Fever Virus Screened From Landscape Phage Display Library. Antiviral Res. 2014; 109:68–71. [PubMed: 24977927]
24. Petrenko VA, Jayanna PK. Phage Protein-Targeted Cancer Nanomedicines. FEBS Letters. 2014; 588:341–349. [PubMed: 24269681]
25. Wang T, Petrenko VA, Torchilin VP. Paclitaxel-Loaded Polymeric Micelles Modified with MCF-7 Cell-Specific Phage Protein: Enhanced Binding to Target Cancer Cells and Increased Cytotoxicity. Mol Pharm. 2010; 7:1007–1014. [PubMed: 20518562]
26. Wang T, Yang S, Mei LA, Parmar CK, Gillespie JW, Praveen KP, Petrenko VA, Torchilin VP. Paclitaxel-Loaded PEG-PE-Based Micellar Nanopreparations Targeted with Tumor-Specific Landscape Phage Fusion Protein Enhance Apoptosis and Efficiently Reduce Tumors. Mol Cancer Ther. 2014; 13:2864–2875. [PubMed: 25239936]
27. Bedi D, Gillespie JW, Petrenko VA, Ebner A, Leitner M, Hinterdorfer P, Petrenko VA. Targeted Delivery of siRNA Into Breast Cancer Cells via Phage Fusion Proteins. Mol Pharm. 2013; 10:551–559. [PubMed: 23215008]
28. Wang J, Dong B, Chen B, Jiang Z, Song H. Selective Photothermal Therapy for Breast Cancer with Targeting Peptide Modified Gold Nanorods. Dalton Trans. 2012; 41:11134–11144. [PubMed: 22868630]
29. Wang F, Liu P, Sun L, Li C, Petrenko VA, Liu A. Bio-Mimetic Nanostructure Self-Assembled From Au@Ag Heterogeneous Nanorods and Phage Fusion Proteins for Targeted Tumor Optical Detection and Photothermal Therapy. Sci Rep. 2014; 4:6808. [PubMed: 25348392]
30. Petrenko, VA.; Smith, GP. Phage Display in Biotechnology and Drug Discovery. Sidhu, SS.; Geyer, CR., editors. CRC Press; Bo Raton, FL: 2005. p. 1-768.
31. Brigati, JR.; Samoylova, TI.; Jayanna, PK.; Petrenko, VA. Phage Display for Generating Peptide Reagents. In: Coligan, JE.; Dunn, BM.; Speicher, DW.; Wingfield, PT., editors. Current Protocols in Protein Science. Vol. 3. John Wiley & Sons, Inc; New Jersey: 2008. p. 1-27.
32. Mandava S, Makowski L, Devarapalli S, Uzubell J, Rodi DJ. RELIC–a Bioinformatics Server for Combinatorial Peptide Analysis and Identification of Protein-Ligand Interaction Sites. Proteomics. 2004; 4:1439–1460. [PubMed: 15188413]
33. Huang J, Ru B, Zhu P, Nie F, Yang J, Wang X, Dai P, Lin H, Guo F-B, Rao N. MimoDB 2.0: a Mimotope Database and Beyond. Nucleic Acids Res. 2012; 40:D271–D277. [PubMed: 22053087]
34. Fagbohun OA, Bedi D, Grabchenko NI, DeInnocentes PA, Bird RC, Petrenko VA. Landscape Phages and Their Fusion Proteins Targeted to Breast Cancer Cells. Protein Eng Des Sel. 2012; 25:271–283. [PubMed: 22490956]
35. Petrenko VA, Smith GP. Phages From Landscape Libraries as Substitute Antibodies. Protein Eng. 2000; 13:589–592. [PubMed: 10964989]
36. Bedi D, Gillespie JW, Petrenko VA. Selection of Pancreatic Cancer Cell-Binding Landscape Phages and Their Use in Development of Anticancer Nanomedicines. Protein Eng Des Sel. 2014; 27:235–243. [PubMed: 24899628]
37. Gross AL, Gillespie JW, Petrenko VA. Promiscuous Tumor Targeting Phage Proteins. Protein Eng Des Sel. 2016; 29:93–103. [PubMed: 26764410]
38. Corti A, Curnis F, Arap W, Pasqualini R. The Neovasculature Homing Motif NGR: More Than Meets the Eye. Blood. 2008; 112:2628–2635. [PubMed: 18574027]
39. Jayanna PK, Bedi D, DeInnocentes PA, Bird RC, Petrenko VA. Landscape Phage Ligands for PC3 Prostate Carcinoma Cells. Protein Eng Des Sel. 2010; 23:423–430. [PubMed: 20185523]
40. Wang T, Yang S, Petrenko VA, Torchilin VP. Cytoplasmic Delivery of Liposomes Into MCF-7 Breast Cancer Cells Mediated by Cell-Specific Phage Fusion Coat Protein. Mol Pharm. 2010; 7:1149–1158. [PubMed: 20438086]
41. Gillespie JW, Gross AL, Puzyrev AT, Bedi D, Petrenko VA. Combinatorial Synthesis and Screening of Cancer Cell-Specific Nanomedicines Targeted via Phage Fusion Proteins. Front Microbiol. 2015; 6:628. [PubMed: 26157433]

42. Zang L, Shi L, Guo J, Pan Q, Wu W, Pan X, Wang J. Screening and Identification of a Peptide Specifically Targeted to NCI-H1299 From a Phage Display Peptide Library. Cancer Lett. 2009; 281:64–70. [PubMed: 19327883]

43. Oyama T, Sykes KF, Samli KN, Minna JD, Johnston SA, Brown KC. Isolation of Lung Tumor Specific Peptides From a Random Peptide Library: Generation of Diagnostic and Cell-Targeting Reagents. Cancer Lett. 2003; 202:219–230. [PubMed: 14643452]

44. Oyama T, Rombel IT, Samli KN, Zhou X, Brown KC. Isolation of Multiple Cell-Binding Ligands From Different Phage Displayed-Peptide Libraries. Biosens Bioelectron. 2006; 21:1867–1875. [PubMed: 16386888]

45. Knez K, Noppe W, Geukens N, Janssen KPF, Spasic D, Heyligen J, Vriens K, Thevissen K, Cammue BPA, Petrenko VA, Ulens C, Deckmyn H, Lammertyn J. Affinity Comparison of P3 and P8 Peptide Displaying Bacteriophages Using Surface Plasmon Resonance. Anal Chem. 2013; 85:10075–10082. [PubMed: 24079816]

46. Koutsioumpa M, Papadimitriou E. Cell Surface Nucleolin as a Target for Anti-Cancer Therapies. Recent Pat Anticancer Drug Discov. 2014; 9:137–152. [PubMed: 24251811]

47. Koivunen E, Wang B, Ruoslahti E. Phage Libraries Displaying Cyclic Peptides with Different Ring Sizes: Ligand Specificities of the RGD-Directed Integrins. Biotechnology. 1995; 13:265–270. [PubMed: 9634769]

48. Maheshwari G, Brown G, Lauffenburger DA, Wells A, Griffith LG. Cell Adhesion and Motility Depend on Nanoscale RGD Clustering. J Cell Sci. 2000; 113:1677–1686. [PubMed: 10769199]

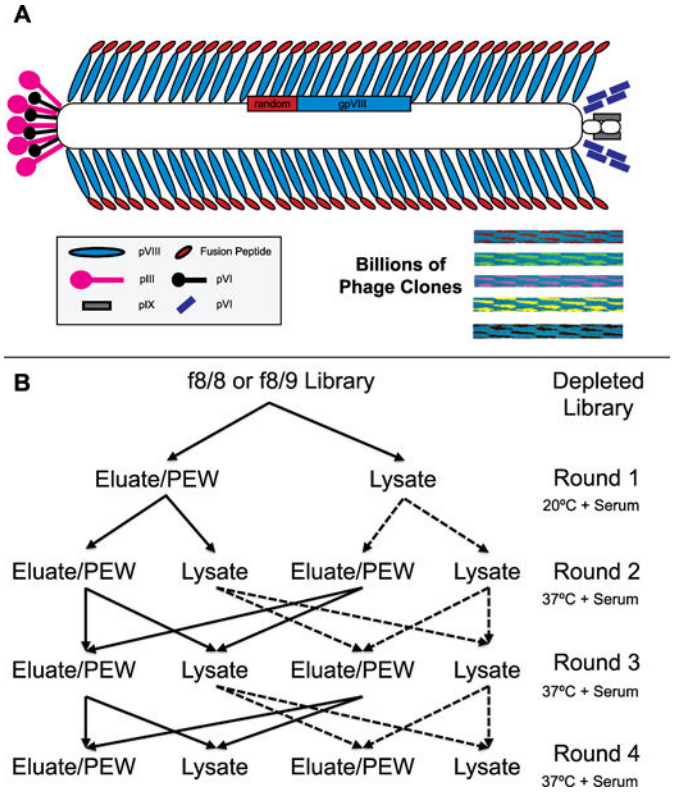


**Figure 1.**

(A) Schematic of f8 type landscape phage display libraries. Diverse fusion derivatives of filamentous phage fd-tet from f8/8 and f8/9 libraries consist of phage with dimensions of 1.2 μm × 6.5 nm and contain a randomized peptide (red) fused to every copy of the N-terminus of the major coat protein pVIII (blue). The major coat proteins cover the length of the single-stranded DNA accommodated at the core of the phage particle. The ends of phage particles are closed by minor coat proteins pIII, pVI, pIX, & pVI. Phage composed of different random peptide fusions create a library of billions of different phage variants with unique surface landscapes. (B) Selection scheme to identify lung cancer cell-specific phage clones. Two input sublibraries were used beginning with second round, identified as an eluate input (solid line) and a lysate input (dashed line). Each input sublibrary was split into two library fractions consisting of eluate and lysate phage that were amplified as individual fractions. In subsequent rounds of selection, the eluate input sublibrary was prepared by combining the eluate fractions generated from both the eluate and lysate output sublibraries from the previous round of selection. A similar scheme was followed for the lysate input.

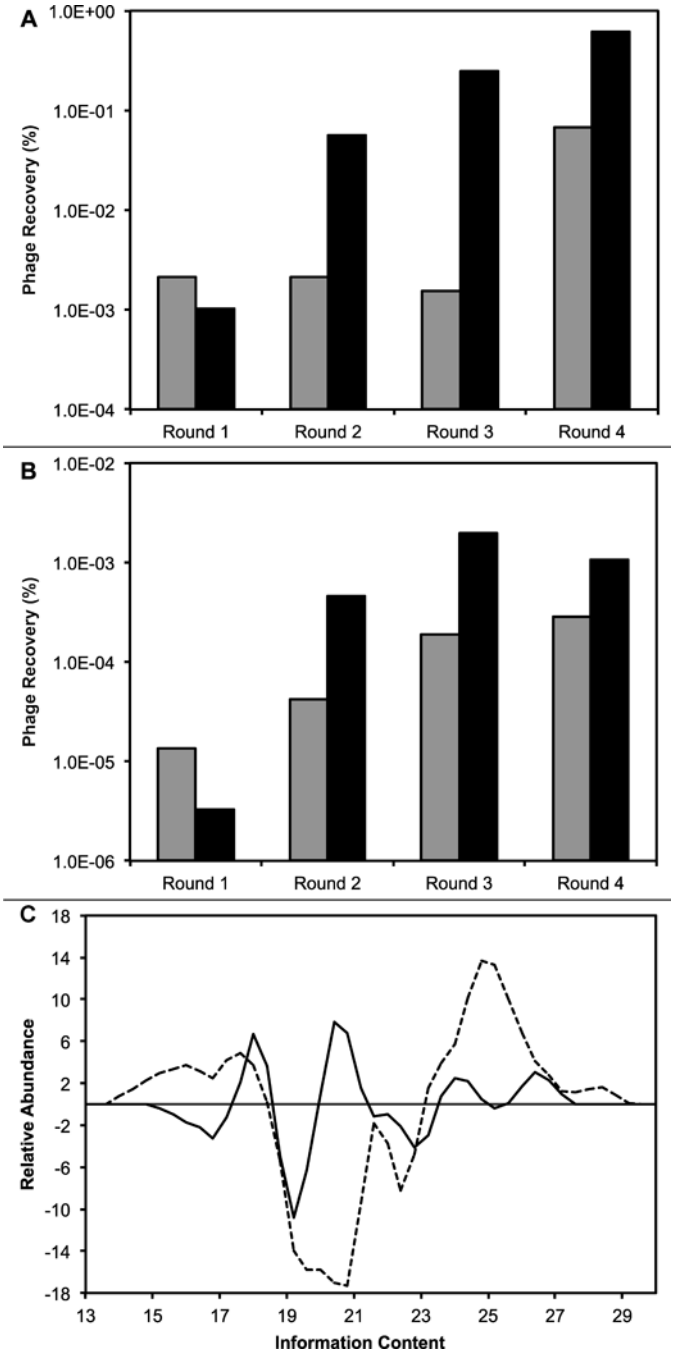


**Figure 2.**

Recovery of phage (output phage/input phage, %) in (A) eluate selection scheme (solid line from Figure 1) and (B) lysate selection scheme (dashed line from Figure 1), isolated from the depleted f8/8 library (gray bars) and f8/9 library (black bars). (C) Histogram of the change in information content available in each sublibrary generated after four rounds of selection against a NSCLC cell line, Calu-3. Information content from clones in f8/8 (black line) and f8/9 (dashed line) are presented. Positive values indicate an increase in total

information content, while negative values indicate a decrease in total information content. More detailed information is given in the results section.

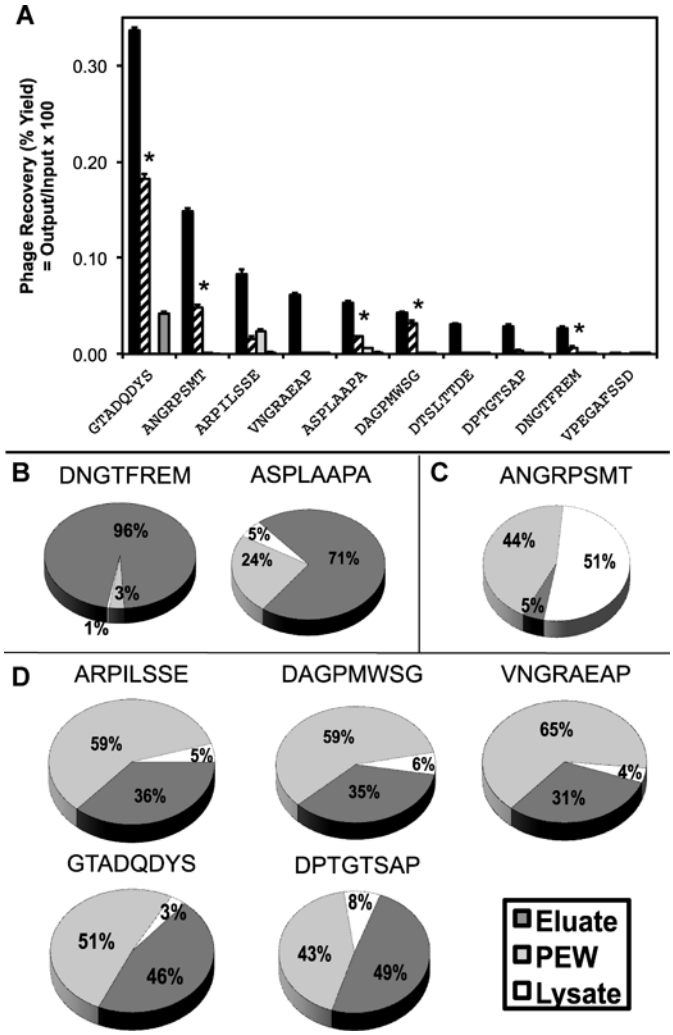


**Figure 3.**

(A) Representative selectivity and specificity assay for select phage clones from the f8/8 library. Individual phage clones were incubated at a constant concentration with: 1) target Calu-3 cells (black), 2) non-related MCF-7 cancer cells (striped), 3) phenotypically normal lung small airway epithelial cells (white), and 4) culture medium with 10% serum (grey). After washing, mammalian cells were lysed and the remaining phage were titered as described in the methods section. Percent recovery was plotted as the number of recovered phage per number of input phage particles for each phage clone. All phage clones binding Calu-3 cells were statistically different from an unrelated phage ($P < 0.0001$) and also different from paired phage samples with different targets ($P < 0.0001$). Phage interactions with MCF-7 cells were compared between paired phage samples with different targets and significant interactions were marked (* $P < 0.0001$). (B–D) Phage mode of interaction with Calu-3 cells after recovery of cell-associated phage by different elution steps with acid and detergent. Cells were split into three general subcellular fractions and the amount of phage associated with each fraction was determined by titering in K91BluKan *E. coli*. The portion of each fraction was calculated as the part of each fraction per total recovered phage. Three

different classes of phage were identified: B) surface bound, C) cytoplasmic, and D) membrane bound.

## Table I
### Families of peptides identified from f8/8 library

Lung cancer-specific phage clones recovered after the fourth round of selection with the f8/8 library in target Calu-3 cells. Phage were grouped into nine different peptide families based on a common consensus sequence (shown in bold) identified between phage clones. Orphan phage clones that did not contain a common consensus sequence between any identified clones were grouped into another family.

| **ASP-----** | **----GTS-** | **V/AD-DYS/T** |
|---|---|---|
| **ASP**LAAPA<br>**ASP**MDVNS | ASLP**GTS**Q<br>DPT**GTS**AP | GT**AD**Q**DYS**<br>**VD**P**DYT**SP |
| **AS/TL----Q** | **--LWS---** | Other |
| **ASL**PGTS**Q**<br>**ATL**WSLG**Q** | AT**LWS**LGQ<br>A**LWS**DSGA | ANEHPMSQ<br>DAGPMWSG<br>DNGTFREM<br>DTSLTTDE<br>EMSYNADA<br>ETMMPYGT<br>VTDPSAST |
| **----EPGQ** | **-NGRP--** | |
| AMLM**EPGQ**<br>ATLM**EPGQ**<br>VTIP**EPGQ**<br>ATVI**EPG**E<br>VTGH**EPG**E | V**NGR**AEAP<br>A**NGRP**SMT<br>A**NGRP**THL<br>AT**GRP**THL | |
| **---FSG--** | **--P-LS-E** | |
| APG**FSG**QP<br>DNP**FSG**TQ | AR**P**I**LS**S**E**<br>GT**P**L**LS**P**E** | |

## Table II
### Families of peptides identified from f8/9 library

Lung cancer-specific phage clones recovered after the fourth round of selection with the f8/9 library in target Calu-3 cells. Phage were grouped into sixteen different peptide families based on a common consensus sequence (shown in bold) identified between phage clones. Orphan phage clones that did not contain a common consensus sequence between any identified clones were grouped into another family.

| **AP---D-DT** | **-EY-E-VNA** | **------MDQ** | **Other** |
|---|---|---|---|
| **AP**AHEYGYD<br>**AP**MFS**D**H**DT**<br>**AP**YSF**DADT** | A**EYGESVNA**<br>G**EYVELVNA** | ESYPMH**MDQ**<br>GVSYVD**MDQ** | ANDVYLD<br>DIPWYGDES<br>AYDPDLGGD<br>EDARTAAMA<br>ADYDFMVDN<br>DPLAEVTTL<br>DPRVESMSG<br>DYPNEYSSA<br>EFYAESTSL<br>EHVYDEGSN<br>EYSPYAGDT<br>GNATLSSME<br>VDIAEQSTA |
| | **----EYG--** | **----RGD--** | |
| **D/E-S-SYIDQ** | APAH**EYG**YD<br>A**EYG**ESVNA | GLNG**RGD**PD<br>EP**RGDS**LDL | |
| **D**E**SI**S**YIDQ**<br>**D**SSL**SYIDQ**<br>**DAS**FMAV**DQ**<br>**E**GMNYH**IDQ** | **------GDS/M** | **----SYI--** | |
| | DGESWG**GDS**<br>DHVWAE**GDS**<br>DMERYS**GDM**<br>VESGAL**GDM** | DM**SYI**ASED<br>DESI**SYI**DQ<br>DSSL**SYI**DQ | |
| | | **------VDS** | |
| **DGR------** | **---GES---** | G**VDS**EIVSL<br>VGDYDV**VDS** | |
| **DGR**DHDAEN<br>**DGR**FDSETS<br>**DGR**SYTGED<br>V**DGR**TGTDS | AEY**GES**VNA<br>D**GES**WGGDS<br>DWMPVE**GES** | | |
| **----EASTL** | **GYD--L---** | **---VEE---** | |
| ADTS**EASTL**<br>EIDP**EASTL** | **GYD**FN**L**TDQ<br>**GYD**LD**L**NAD | EVN**VEE**INL<br>**VEE**GGYIAA | |
| **---EPGL--** | **GSLEE-S-L** | | |
| EPF**EPGL**AS<br>GMVM**EPGL**D | **GSLEE**V**S**T**L**<br>**GSLEE**SS**NL** | | |

## Table III

### Selectivity of Select Lung Cancer Clones

Representative selectivity data for select phage clones from the f8/9 library. Information content refers to a statistic generated by RELIC comparing the probability of amino acid occurrence in a selected clone compared to an unselected library. Specificity refers to the ability of a clone to identify the target compared to an unrelated clone. Selectivity refers to the ability of a clone to discriminate between two cell types, here Calu-3 cells compared to phenotypically normal lung cells (SAE).

| Phage | Information Content | Specificity | Selectivity (Calu-3/SAE) |
|---|---|---|---|
| EVNVEEINL | 28.245 | 76.91 | 3.31 |
| GEYVELVNA | 26.867 | 145.12 | 2.40 |
| GMVMEPGLD | 26.092 | 62.49 | 2.29 |
| GVSYVDMDQ | 25.452 | 119.53 | 1.15 |
| AEYGESVNA | 25.054 | 48.11 | 1.73 |
| DESISYIDQ | 25.029 | 24.04 | 14.01 |
| VPEGAFSSD | – | 2.23 | 4.11 |